Biological Psychiatry

Archival Report

Chronic Stress Induces Coordinated Cortical Microcircuit Cell–Type Transcriptomic Changes Consistent With Altered Information Processing

Dwight F. Newton, Hyunjung Oh, Rammohan Shukla, Keith Misquitta, Corey Fee, Mounira Banasr, and Etienne Sibille

ABSTRACT

BACKGROUND: Information processing in cortical cell microcircuits involves regulation of excitatory pyramidal (PYR) cells by inhibitory somatostatin- (SST), parvalbumin-, and vasoactive intestinal peptide–expressing interneurons. Human postmortem and rodent studies show impaired PYR cell dendritic morphology and decreased SST cell markers in major depressive disorder or after chronic stress. However, knowledge of coordinated changes across microcircuit cell types is virtually absent.

METHODS: We investigated the transcriptomic effects of unpredictable chronic mild stress (UCMS) on distinct microcircuit cell types in the medial prefrontal cortex (cingulate regions 24a, 24b, and 32) in mice. C57BL/6 mice, exposed to UCMS or control housing for 5 weeks, were assessed for anxiety- and depressive-like behaviors. Microcircuit cell types were laser microdissected and processed for RNA sequencing.

RESULTS: UCMS induced predicted elevations in behavioral emotionality in mice. DESeq2 analysis revealed unique differentially expressed genes in each cell type after UCMS. Presynaptic functions, oxidative stress response, metabolism, and translational regulation were differentially dysregulated across cell types, whereas nearly all cell types showed downregulated postsynaptic gene signatures. Across the cortical microcircuit, we observed a shift from a distributed transcriptomic coordination across cell types in control mice toward UCMS-induced increased coordination between PYR, SST, and parvalbumin cells and a hub-like role for PYR cells. Finally, we identified a microcircuit-wide coexpression network enriched in synaptic, bioenergetic, and oxidative stress response genes that correlated with UCMS-induced behaviors.

CONCLUSIONS: These findings suggest cell-specific deficits, microcircuit-wide synaptic reorganization, and a shift in cells regulating the cortical excitation–inhibition balance, suggesting increased coordinated regulation of PYR cells by SST and parvalbumin cells.

https://doi.org/10.1016/j.biopsych.2021.10.015

Major depressive disorder (MDD) is a severe psychiatric disorder, characterized by low mood, anhedonia, and cognitive dysfunction, affecting 300 million people annually (1,2). Monoaminergic antidepressants have poor response rates (50%), resulting in a substantial gap in treatment, necessitating novel antidepressant modalities (3). Moreover, given the neuronal diversity of the brain (4) and the burgeoning understanding of cell-specific pathologies in MDD, a refined understanding of its neurobiology and novel potential antidepressant targets is required (5).

Cortical brain regions, implicated in MDD pathophysiology, are characterized by a repeated, phylogenetically conserved neuronal microcircuitry, consisting of glutamatergic pyramidal (PYR) cells, regulated by diverse inhibitory GABAergic (gamma-aminobutyric acidergic) interneurons (Figure 1A) (5,6). Somatostatin (SST)-expressing cells innervate distal PYR cell dendrites and regulate corticocortical and thalamocortical inputs (5). Parvalbumin (PV)-expressing cells innervate the soma and axon hillock of PYR cells, regulating output (5). Vasoactive intestinal peptide (VIP)–expressing cells innervate SST cells, disinhibiting PYR cells (5). PYR cell projections onto each interneuron population mediate feedback inhibition, creating an interconnected structure with inherent excitation–inhibition balance (EIB). EIB reflects the balanced strength, or activity, of GABAergic and glutamatergic synapses and cell types (7), which are required for accurate information processing. We described elsewhere how altered cell type–specific function may impair information processing and corrupt the cortical microcircuit–mediated neural code (8). This controlled balance also suggests that acute and chronic transcriptional changes within cells are likely coordinated across cell types.

The anterior cingulate cortex (ACC), a mood-regulating brain region, shows elevated activity during depressive episodes, which normalizes with successful antidepressant therapy (9). EIB disruptions manifest in vivo in MDD as cortical inhibitory deficits, namely decreased $GABA_A$ and $GABA_B$

SEE COMMENTARY ON PAGE 770

 © 2021 Society of Biological Psychiatry.
 ISSN: 0006-3223

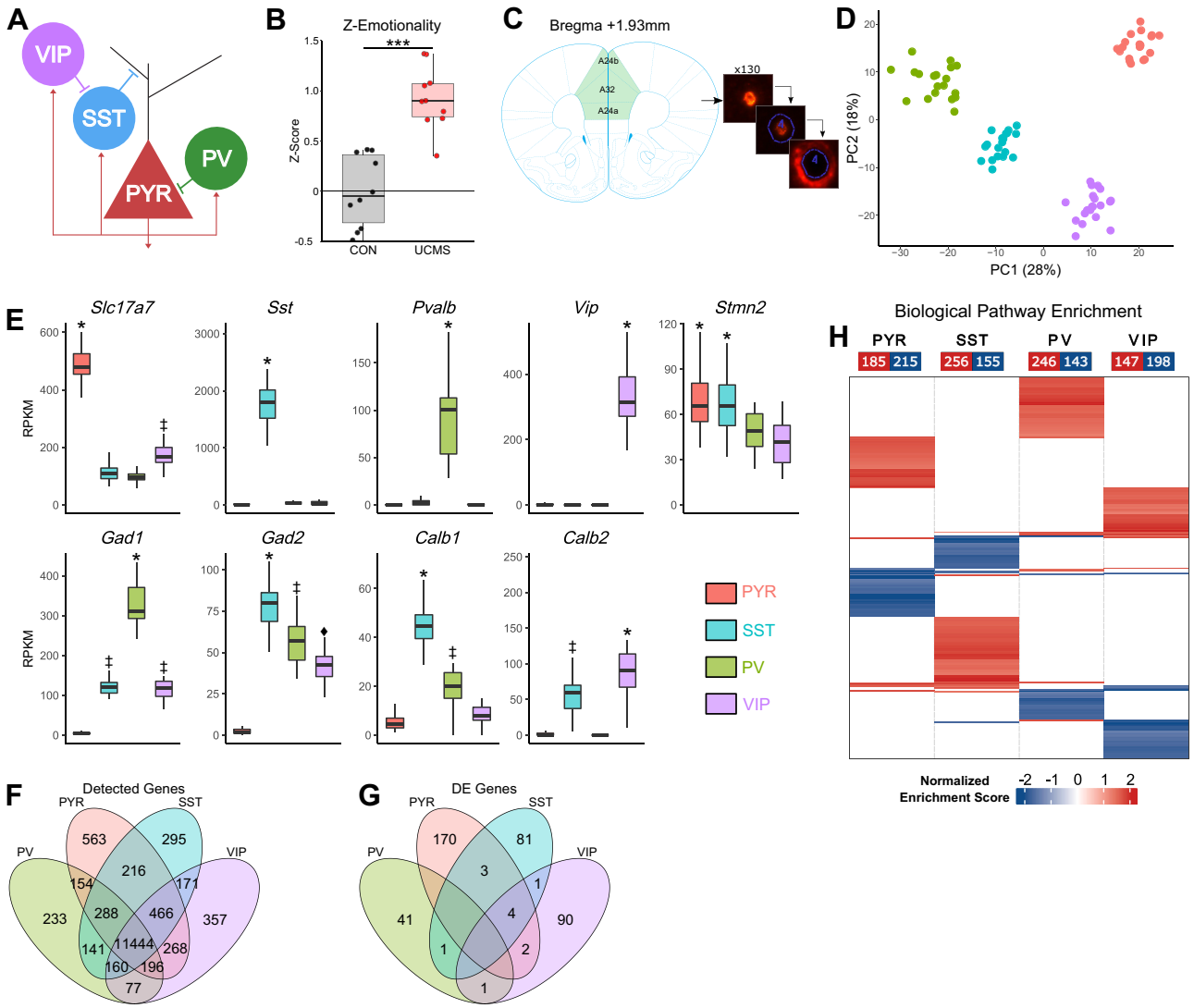

Figure 1. Isolated microcircuit cell types show expected enrichment of molecular markers and cell-specific transcriptomic perturbations. **(A)** Schematic of the canonical cortical cell microcircuit and connectivity patterns. PYR cells (red) are excitatory glutamatergic cells, regulated by different GABAergic interneurons. SST-expressing cells (blue) synapse onto PYR cell dendrites, providing continuous tonic inhibitory tone. PV-expressing cells (green) synapse onto perisomatic regions and the axon hillock of PYR cells and other PV cells (not shown) to provide phasic inhibition and synchrony of PYR cell firing across cortical microcircuit columns. VIP-expressing cells (violet) synapse onto SST cells, regulating their activity and contributing to the integration of corticocortical and thalamocortical inputs onto PYR cell dendrites and VIP cells. PYR cells form synapses onto each interneuron cell type, mediating feedback inhibition. **(B)** Behavioral emotionality *z* scores in CON (black) and UCMS-exposed (red) mice. Emotionality is significantly increased ($p = 7.41 \times 10^{-6}$) in UCMS-exposed mice. **(C)** Delineation of brain regions from which 130 of each microcircuit cell type were extracted. The laser capture microdissection workflow is visualized, in which a VIP cell (red fluorescence, image 1) is identified and the laser path is manually traced (blue outline). A space between the cell and laser path prevents the laser from directly damaging cellular contents (image 2). After laser dissection, a halo surrounding the area previously occupied by the cell results from the reaction of the tissue to the laser (image 3). **(D)** Principal component analysis of omnibus gene expression in PYR, SST, PV, and VIP cells. K-means clustering (k = 4) confirms that the cell types form exclusive clusters. **(E)** Enrichment of cell-type molecular marker expression. *, ‡, and ◇ indicate $p < 1 \times 10^{-4}$ vs. those without the same symbol. **(F)** Venn diagram of number of genes detected across cell types. **(G)** Venn diagram of number of significantly differentially expressed ($p < .05$, $|\log_2$ fold-change$| > 20\%$) genes across cell types. **(H)** Heatmap showing significantly enriched ($p < .05$) biological pathways in each cell type, shaded by normalized enrichment score (blue: downregulated, red: upregulated). CON, control; DE, differentially expressed; GABAergic, gamma-aminobutyric acidergic; PC, principal component; PV, parvalbumin; PYR, pyramidal; RPKM, reads per kilobase of transcript per million reads mapped; SST, somatostatin; UCMS, unpredictable chronic mild stress; VIP, vasoactive intestinal peptide.

receptor–mediated inhibition and GABA reductions in cortical brain regions (10,11). Decreased expression of GABAergic and glutamatergic synaptic genes was reported in transcriptomic studies of MDD (12–14). Technical limitations have limited large-scale transcriptomic profiles to bulk tissue assays, masking cell type–specific effects, and recent single-nucleus RNA sequencing (RNA-seq) studies have not assessed the subgenual ACC (15). Targeted investigations of cell type–

specific molecular markers have repeatedly identified reduced SST expression in the ACC and prefrontal cortex (PFC) in MDD (16–18). This reduction manifested as reduced expression per cell, suggesting impaired SST cell function (17).

Insights into cellular bases of EIB disruptions in MDD have come from mouse stress models, including unpredictable chronic mild stress (UCMS), a paradigm that recapitulates behavioral and neurobiological phenotypes reminiscent of MDD (8,19,20). UCMS-exposed mice show reduced SST expression and increased signaling of the unfolded protein response in SST cells, indicating compromised proteostasis (17,21). These deficits suggest impaired SST-mediated inhibition, such as reduced filtering of spurious excitatory inputs and altered PYR cell signal-to-noise ratio, leading to impaired processing of mood-relevant information. This is consistent with SST cells providing a blanket of inhibition across PYR cells (22), which is impaired when SST cell function is compromised (23). Indeed, SST knockout mice show elevated depressive-like behavior, suggesting a causal link between SST and depression (21). UCMS studies report evidence of PYR cell deficits, namely reduced spine density, dendritic atrophy, and synapse loss (24–26). PYR cells also show reduced expression of postsynaptic glutamatergic markers after UCMS (26,27). However, these cellular deficits occur in the context of cortical microcircuitry, and the concurrent changes in PV and VIP cells are understudied (28). Moreover, the coordinated changes occurring across the microcircuitry in either MDD or UCMS, even between SST and PYR cells, have been inferred from disparate studies and not studied in combination (8,24,29).

Stress represents a potential origin for these cellular deficits, given its salience in precipitating depressive episodes and the similarity of UCMS and MDD on multiple investigational levels. Moreover, UCMS provides an environment to study early pathological changes occurring over weeks, versus years, of MDD disease burden (30). We hypothesized that UCMS induces coordinated transcriptomic changes within and across microcircuit cell types and that some of these cellular and molecular changes are related to anxiety- and depressive-like behaviors. To test this hypothesis, we used laser capture microdissection to harvest microcircuit cell types from the medial PFC, roughly homologous to the ACC in humans (31). RNA-seq was used to obtain cell type–specific, transcriptome-wide, gene expression profiles in mice exposed to UCMS versus control animals. We predicted that previously observed markers of functional and/or structural deficits in SST and PYR cells would be replicated, cell types would show unique transcriptional profiles in response to UCMS, and changes would be coordinated across cell types, reflecting altered cellular communication and information processing.

METHODS AND MATERIALS

See Supplement 1 for detailed materials and methods.

A total of 20 male C57BL/6J mice were exposed to control or UCMS conditions (n = 10/group) for 5 weeks and were tested for anxiety- and anhedonia-like behaviors, as described previously (30). All procedures were approved by the Centre for Addiction and Mental Health Animal Care Committee and are in accordance with the Canadian Animal Care Committee. A total of 130 cells of each cell type (PYR, SST, PV, and VIP neurons) were collected per mouse from the cingulate areas 24a, 24b, and 32 using fluorescent in situ hybridization and laser capture microdissection (32). RNA-seq was performed (33) using the HiSeq 2500 platform (Illumina). Differential expression (DE), gene set enrichment analysis, and weighted gene coexpression analysis were used to assess transcriptomic changes within and across cell types (34–36). DE significance was set at 15% false discovery rate and gene-set enrichment analysis significance at $p < .05$ (21,33,37–39).

RESULTS

UCMS-Exposed Mice Exhibit Elevated Behavioral Emotionality

Mice exposed to 5 weeks of UCMS exhibited the expected increase in behavioral emotionality ($p = 7.41 \times 10^{-6}$), an omnibus measure of behavior test scores related to anxiety- and depression-like behaviors (Figure 1B). Figure S1 in Supplement 1 outlines all behavioral test results.

RNA-Seq Reveals Robust and Microcircuit Cell Type–Specific Gene Enrichment Profiles

Cell-type densities were unchanged in UCMS (Figure S2 in Supplement 1). RNA-seq of laser capture microdissection–collected cells (Figure 1C) revealed robust cell type–specific clustering (100% accuracy: k-means clustering, k = 4) using principal component analysis (Figure 1D). Cell types showed expected enrichments of molecular markers (all $p < 1 \times 10^{-4}$) (Figure 1E): *Slc17a7*, *Sst*, *Pvalb*, and *Vip* in their respective cell types; *Gad1* (GAD67) and *Gad2* (GAD65) exclusively in interneurons; *Calb1* (calbindin) in SST and PV cells and *Calb2* (calretinin) in SST and VIP cells; and *Stmn2*, a pan-neuronal marker, in all cell types. Overall, 13,429 genes were detected above expression thresholds in PYR cells, 13,060 in SST cells, 12,047 in PV cells, and 13,065 in VIP cells, with 11,159 expressed in all cell types (Figure 1F).

UCMS Induces Microcircuit Cell Type Unique Biological Changes

DESeq2 analysis yielded 179 DE genes (79 upregulated, 100 downregulated) in PYR cells, 90 genes (42 upregulated, 48 downregulated) in SST cells, 43 genes (16 upregulated, 27 downregulated) in PV cells, and 98 genes (44 upregulated, 54 downregulated) in VIP cells, which were largely unique to each cell type (Figure 1G) (gene lists in Table S1 in Supplement 2). Analysis of altered biological pathways using gene set enrichment analysis identified 400 biological pathways enriched in PYR cells (185 upregulated, 215 downregulated), 411 pathways in SST cells (256 upregulated, 155 downregulated), 389 pathways in PV cells (246 upregulated, 143 downregulated), and 345 pathways in VIP cells (147 upregulated, 198 downregulated) (Figure 1H). These results were summarized using unbiased clustering of biological pathways (Figure 2; Table S2 in Supplement 2), in parallel with investigations of biological functions with a priori links to MDD and UCMS (Supplemental Methods and Figure S2 in Supplement 1). Results are described next for each cell type,

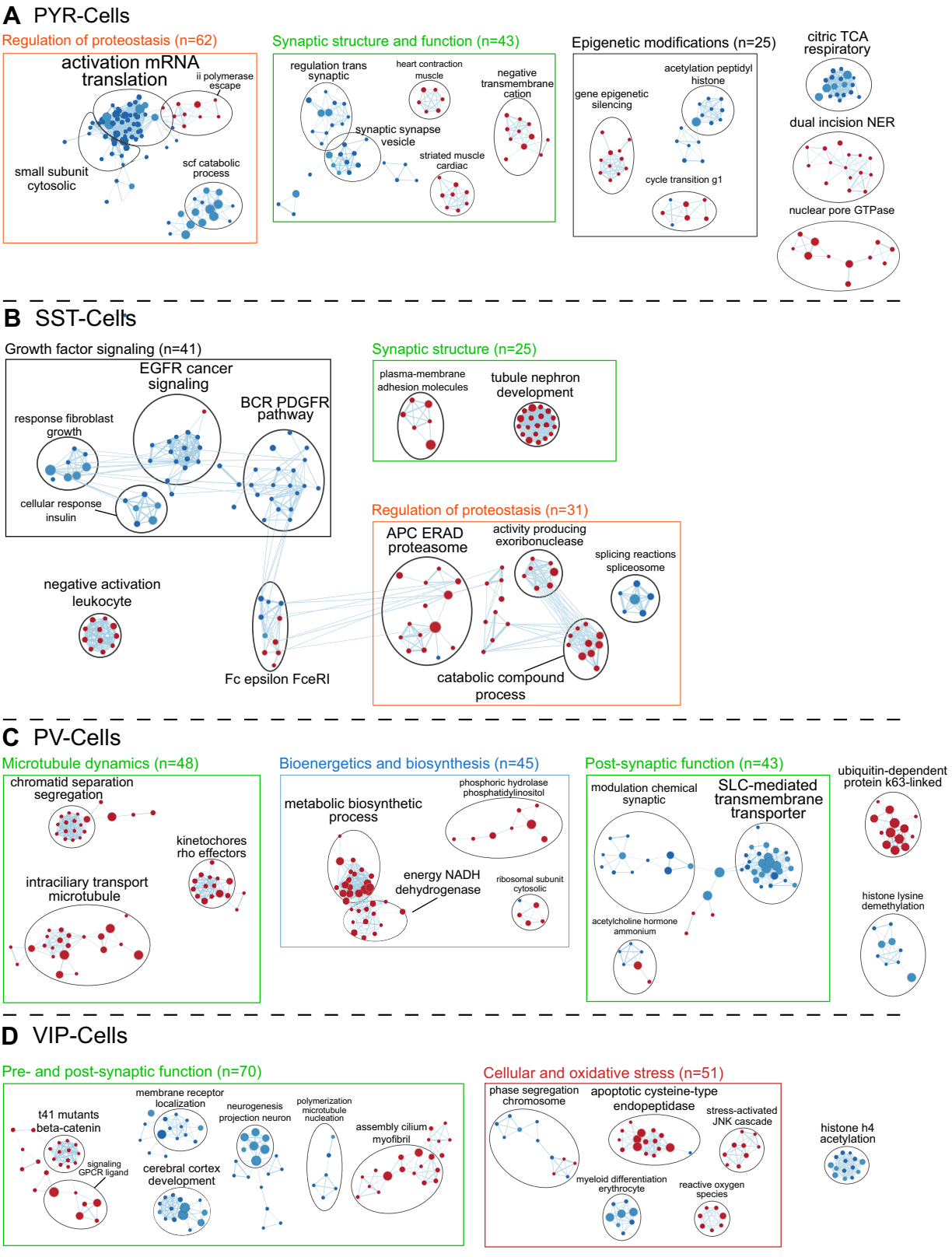

Figure 2. Cluster-based visualization of biological pathways altered by UCMS shows cell-specific profiles of synaptic, bioenergetic, and proteostasis deficits. EnrichmentMap networks displaying gene set enrichment analysis results for **(A)** PYR cells, **(B)** SST cells, **(C)** PV cells, and **(D)** VIP cells. Nodes

with significant DE genes driving enrichment across multiple pathways highlighted for context.

PYR Cells. Three clusters representing 62 pathways, associated with the regulation of proteostasis, encompassing translational machinery and initiation, proteasome, and autophagy, showed downregulation (Figure 2A; Table S3 in Supplement 2). These changes were driven by *Psmb6*, *Ubb*, and *Rplp0*, three genes associated with protein translation and quality control, downregulated in UCMS, and enriched across multiple clustered pathways (full list in Table S3 in Supplement 2). Five clusters (43 pathways) were associated with synaptic structure and function. These clusters were characterized by downregulation of neurotransmitter release driven by presynaptic (*Cplx1*) and postsynaptic (*Grin2d*, *Nos1*) genes and upregulated inhibition of ion transporters and glutamatergic signaling (*Homer1*). Three clusters (25 pathways) associated with epigenetic modifications were both up- and downregulated, although no significant DE genes drove these findings. One cluster (18 pathways) associated with bioenergetics (*citric tca respiratory*) showed downregulation of oxidative phosphorylation, primarily cytochrome *c* subunits (*Cox5a* and *Cox7b*). Enrichment of a priori biological functions was consistent with cluster-based results, implicating altered synaptic transmission and stress-related pathways (Figure S3 in Supplement 1).

To support findings of reduced postsynaptic receptor expression in PYR cells, we independently validated altered *Grin2d* in PYR cells using RNAscope (Figure 3). RNA-seq identified reduced *Grin2d* expression in UCMS ($\log_2$ fold change = -1.34, $q = 2.7 \times 10^{-4}$), with RNAscope results confirming significantly fewer messenger RNA (mRNA) grains in PYR cells after UCMS ($\log_2$ fold change = -0.51, $p = 1.0 \times 10^{-14}$).

Overall, these results suggest decreased PYR cell excitatory function, evidenced by downregulation of synaptic structure and function genes, compromised proteostasis, and reduced mitochondrial function. Suggested consequences at the microcircuitry information processing level include reduced PYR-mediated information output and reduced feedback activation of local inhibitory cells.

SST Cells. Four clusters (41 pathways) associated with growth factor and neurotrophic signaling pathways, namely insulin, epidermal growth factor, fibroblast growth factor (FGF), and platelet-derived growth factor, were downregulated in SST cells of UCMS-exposed mice (Figure 2B; Table S4 in Supplement 2). Four clusters (31 pathways) associated with proteostasis, characterized by response to endoplasmic reticulum (ER) stress, were upregulated. These pathways were driven by proteasome, chaperone (*Hspa5* and *Tor1a*), and mRNA degradation genes (*Eri1* and *Pde5a*). Two clusters (25 pathways) associated with synaptic structure, including postsynaptic cadherin-mediated adhesion (*Smad4*, *Celsr1*, *Clstn2*, and *Ctnnd1*), were also upregulated. Finally, enriched a priori functions were consistent with those described above (Figure S3 in Supplement 1), including upregulated synapse structure, stress-related pathways, cell adhesion molecules (CAMs) driven by cadherin-binding proteins, and ER stress (*Hspa5*). SST cell findings were overall less robust than PYR cells, with all genes identified at a 25% false discovery rate but not at a 15% false discovery rate.

Overall, these results suggest decreased SST cell function, evidenced by reduced growth factor and neurotrophic support, altered proteostasis, and increased ER stress (primarily translational inhibition). These predicted impairments would contribute to reduced input regulation of incoming excitatory inputs onto PYR cells.

PV Cells. Pathway-level findings in PV cells are tentative, because fewer significant DE genes were identified, and leading-edge analyses identified only three DE genes driving enrichment across multiple pathways within clusters (Figure 2C; Table S5 in Supplement 2). As such, these findings must be held to a lower degree of confidence than findings in other cell types, although many pathways were significantly enriched regardless.

Three clusters (48 pathways) associated with microtubule dynamics were upregulated in PV cells of UCMS-exposed mice. These clusters were characterized by increased axonal microtubule polymerization, stabilization, and anterograde transport (*Exoc5*) and inhibition of retrograde transport along microtubules. Four clusters (45 pathways) associated with bioenergetics and biosynthesis were upregulated, driven by genes involved in glycolysis (*Gpd1*), oxidative phosphorylation, and nucleotide biosynthesis. Finally, three clusters (43 pathways) associated with postsynaptic functions were downregulated, including glutamatergic (*Kcnk9*) and cholinergic signaling and postsynaptic CAMs. A priori function enrichment resembled cluster-based results, suggesting upregulation of ER stress– and bioenergetics-related pathways and downregulation of synaptic-related pathways (Figure S3 in Supplement 1), particularly potassium channels (*Kcnk9*).

Overall, the PV cell results suggest increased neuronal and cellular bioenergetic activities and decreased glutamatergic and cholinergic signaling input, with the caveat of low statistical confidence in these findings. These findings would suggest an increased or intact PV cell function, contributing to

indicate gene sets (pathways), with node size representing the number of genes. Edges indicate the similarity of gene sets calculated by a 50:50 ratio of the Overlap and Jaccard indices. Red and blue indicate up- and downregulation, respectively. Clusters defined by Markov clustering were named based on semantic similarity of gene set names (using the AutoAnnotate Cytoscape package). Because cluster names are based on gene set names, spurious non-neuronal functions can occur (e.g., tubule nephron development) and are further characterized by examining shared functions and leading-edge genes. Green boxes indicate clusters related to altered synaptic functions, orange indicates proteostasis and autophagy, blue indicates bioenergetics, red indicates cellular stress, and black indicates functions altered in only one cell type. Bracketed numbers indicate the total number of gene sets in the group of clusters. APC, anaphase-promoting complex; BCR, breakpoint cluster region; EGFR, epidermal growth factor receptor; ERAD, endoplasmic reticulum–associated degradation; GTP, guanosine triphosphate; mRNA, messenger RNA; NADH, nicotinamide adenine dinucleotide; NER, nucleotide excision repair; PDGFR, platelet-derived growth factor receptor; PV, parvalbumin; PYR, pyramidal; SLC, solute carrier; SST, somatostatin; TCA, tricarboxylic acid; UCMS, unpredictable chronic mild stress; VIP, vasoactive intestinal peptide.

increased or equivalent output regulation of PYR cells in UCMS.

VIP Cells. VIP cells showed bidirectional enrichment in seven clusters (70 pathways) associated with synaptic structure and function and suggesting complex cytoskeletal reorganization of axons and dendrites (Figure 2D; Table S6 in Supplement 2). This included downregulated neurotrophic factor signaling relevant to cytoskeletal maintenance (*Arsb*, *Nfasc*, *Nf2*) and postsynaptic CAMs (*Stx1b*). Five clusters (51 pathways) associated with cellular and oxidative stress showed mixed patterns, with decreased regulation and activity of autophagosomes, increased MAPK (mitogen-activated protein kinase) signaling, increased oxidative stress response, and increased ER stress response (*Bcap31*). Cellular stress findings showed only one leading-edge gene driving enrichment across multiple pathways, whereas many were observed for synaptic clusters, indicating greater confidence in synaptic changes than cellular stress.

A priori functions (Figure S3 in Supplement 1) showed consistent downregulation of synaptic pathways and upregulation of cellular stress pathways. Downregulated synaptic structure pathways were reflective of decreased postsynaptic complexes and axonal growth and function (*Ank1*, *Nfasc*). Stress pathways reflected modestly upregulated response to reactive oxygen species (ROS) and apoptotic signaling through MAPK pathways.

Overall, the VIP cell results suggest potential atrophy or reorganization of axonal and postsynaptic compartments, combined with increased oxidative and other cellular stressors. The functional consequences would suggest decreased VIP cell integrity and function, implicating impaired regulation of SST cells in response to incoming excitatory inputs.

UCMS Strengthens Gene Coexpression Patterns Between PYR Cells and SST/PV Cells

We next used weighted gene coexpression analysis to explore putative coordinated changes across microcircuitry cell types in response to UCMS and coexpression signatures of UCMS-induced behavior (Figure 4A). We identified coexpression modules within individual cell types and explored correlation between these modules across cell types. Overall, 26 to 33 gene coexpression modules were identified per cell type under control or UCMS conditions (Table S7 in Supplement 2) and summarized by their representative eigengene value. In control mice, eigengene coexpression networks revealed a balanced pattern of correlated modules, suggesting a homogeneous equilibrium across cell types (Figure 4B). In UCMS, a marked shift was observed, with significantly increased module coexpression between PYR and PV cells ($p = 1.0 \times 10^{-4}$) and between PYR and SST cells ($p = .029$), whereas correlations between PYR and VIP cells were not significantly different ($p = .42$).

These results demonstrate transcriptome-wide coexpression between SST, PYR, and PV cells after UCMS, implicating these cell types as the key locus of UCMS response. Combined with the cell type–specific functional analyses, these results suggest decreased SST cell–mediated regulation of PYR cell input, decreased PYR cell signaling, and increased PV cell regulation of PYR cell output, together maintaining the EIB, albeit with negative consequences for information processing.

Gene Coexpression Modules Relevant to UCMS-Induced Behavior Suggest a Coordinated Response to Stress Implicating Synaptic Reorganization

Finally, to identify coexpression modules and biological functions correlating with UCMS-induced behaviors, we extracted a subnetwork of modules with significant eigengene correlations with behavioral emotionality *z* scores (Table S8 in Supplement 2). Module gene lists are available in Table S9 in Supplement 2. Few modules correlated with behavioral variability in control mice, which formed a disconnected network (Figure 4C, left). Conversely, a greater, but still small, number of modules were correlated with behavior after UCMS. These modules formed an organized subnetwork linking the four cell types, centered around PYR cells, as detected by increased PYR cell hub–related graph measures (closeness centralization: UCMS = 0.629 vs. control mice = 0.208, $p = 2.86 \times 10^{-5}$; betweenness centralization: UCMS = 0.320 vs. control mice = 0, $p = 2.55 \times 10^{-4}$) (Figure 4C, right). UCMS-associated modules showed enrichment in axonal and dendritic reorganization, bioenergetics, and cellular stress in all cell types (Table S10 in Supplement 2).

Overall, these results implicate PYR cells as a hub cell type, either coordinating a microcircuitry-wide response to UCMS or undergoing altered regulation by SST and PV cells, characterized by cellular stress, altered metabolism, and synaptic reorganization.

DISCUSSION

To our knowledge, this study represents the first simultaneous investigation of cortical microcircuit cell type–transcriptomic changes induced by chronic stress (UCMS), circuit-wide coordinated adaptations, and transcriptional signatures related to UCMS-induced behavior. First, we identified cell type–specific transcriptional signatures after UCMS. Second, presynaptic functions, ROS response, metabolism, and translational regulation were differentially dysregulated across cell types, whereas nearly all cell types showed downregulation of postsynaptic gene signatures. Third, we observed a shift in cellular coordination, in which UCMS increased coexpression between PYR and both SST and PV cells (Figure 4). Finally, we identified a microcircuit-wide coexpression network enriched in genes related to synaptic, bioenergetic, and ROS response that correlated with UCMS-induced behaviors. These findings identify cell type–specific effects of UCMS on the microcircuitry, are consistent with reports showing compromised SST and PYR cell functions (8,24), and identify pathological processes occurring in PV and VIP cells. Overall, this suggests impaired input regulation and intact or increased output regulation of PYR cells, ultimately implicating a maintained microcircuit EIB at a decreased activity and a potentially corrupted mood-relevant information.

Microcircuit-wide Effects of UCMS

Our cell-specific findings suggest a pattern of synaptic reorganization across the microcircuitry in UCMS versus control

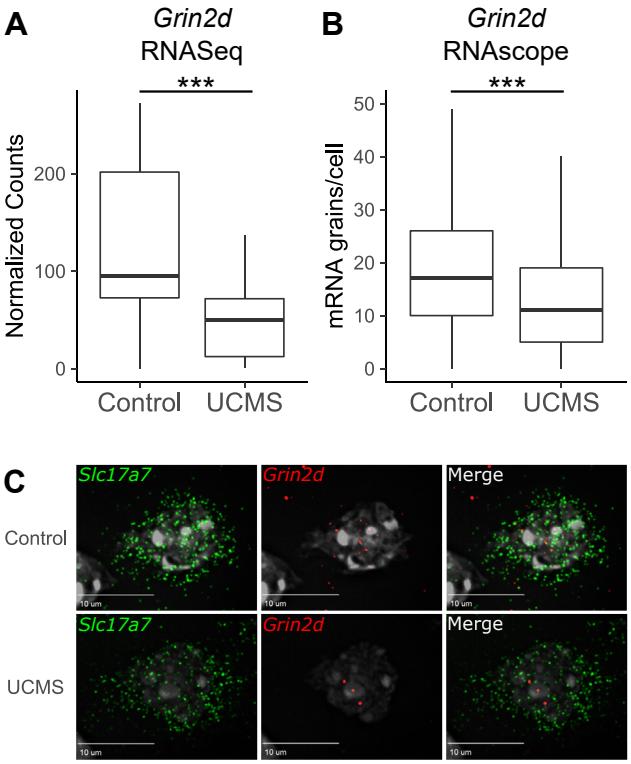

Figure 3. Validation of reduced *Grin2d* in PYR cells. **(A)** Boxplots showing significantly reduced *Grin2d* expression in PYR cells of UCMS-exposed mice as measured by RNA-seq (log_2 fold change = −1.34, $q = 2.7 \times 10^{-4}$). **(B)** Boxplots showing significantly reduced *Grin2d* mRNA grains in PYR cells of UCMS-exposed mice as measured by RNAscope (log_2 fold change = −0.51, $p = 1.0 \times 10^{-14}$). **(C)** Representative 60× confocal microscopy images showing *Grin2d* expression in PYR cells of control mice (upper images) and UCMS-exposed mice (lower images). *Slc17a7* is shown in green, *Grin2d* in red, and DAPI in gray. Scale bar represents 10 μm. *** indicates $q < 0.001$ or $p < .001$, as appropriate. mRNA, messenger RNA; PYR, pyramidal; RNASeq, RNA sequencing; UCMS, unpredictable chronic mild stress.

mice (Figure 5). PYR cell changes suggest decreased glutamatergic inputs onto all cell types, and SST and VIP cell changes suggest decreased inhibition of their respective targets. In contrast, PV cells are the only cell type showing a transcriptomic profile consistent with increased activity. This may represent a compensatory increase in PV cell–mediated inhibition of PYR cell output following decreased SST cell–mediated inhibition of PYR cell inputs to maintain the EIB of the microcircuitry. These results are strengthened by observations of altered mitochondrial function and ROS response across cell types, internally consistent with the respective changes in bioenergetic demand. These results are consistent with extant literature indicating deficient PYR cell structure and function (27,40), loss of SST cell proteostasis and ER stress (21), and decreased GABAergic and glutamatergic function (29). We identify here for the first time that such deficits occur simultaneously.

Our coexpression results provided three primary findings. First, UCMS induces a coordinated set of transcriptomic changes occurring primarily between PYR, PV, and SST cells. This indicates that the integrated response to UCMS is biased toward these cell types, with VIP cell deficits occurring in relative isolation. Indeed, the emotionality-related subnetwork, showing a convergent enrichment profile of biological functions with cell-specific analyses, suggests that synaptic reorganization, oxidative stress response, and oxidative phosphorylation processes occur in a coordinated manner across the microcircuitry. Second, a portion of the cell-specific synaptic, oxidative stress, and bioenergetic disruptions identified in DE analyses are correlated across cell types, consistent with a coordinated response to UCMS across the microcircuitry. Third, PYR cells represented the primary hub cell type in both the metanetwork and subnetwork analyses. This suggests that PYR cells are the putative focal point, but not necessarily the initiating factor, of the response to UCMS within the microcircuit and that the PYR-PV-SST complex is a particularly salient target for potential pharmacotherapy.

Cell Type–Specific Effects of UCMS

A unique transcriptomic profile was observed in each cell type after UCMS, indicating unique responses and/or adaptations to stress. PYR cells showed deficits in glutamatergic signaling, translation, autophagy, and postsynaptic receptor complexes. Deficits in glutamatergic and synaptic functions are internally consistent with observations of decreased postsynaptic glutamatergic receptors and scaffolding expression in PYR, PV, and VIP cells, which all receive PYR cell inputs (5). This suggests pervasive pre- and postsynaptic deficits in PYR cells across multiple efferent cellular targets, consistent with previous reports of reduced PYR cell synapses in UCMS and reduced PYR cell function (40). Reduced mitochondrial function in PYR cells is also largely consistent with extant UCMS literature (41,42). Autophagy and proteostasis deficits indicate reduced subcellular component quality control and turnover critical for synaptic plasticity and the regulation of synaptic vesicles and postsynaptic GABA and NMDA receptors (43,44). Autophagic deficits can alter PYR cell activity through altered trafficking of postsynaptic receptors (45). This may indicate a potential antidepressant modality, given that the rapid-acting antidepressant ketamine increases autophagy (46) and dendritic spine regeneration (47). Overall, the PYR cell findings, consistent with existing UCMS literature, suggest reduced PYR cell activity in UCMS.

SST cells were characterized by reduced growth factor signaling and upregulation of presynaptic CAMs and response to ER stress after UCMS. ER stress induced adaptive responses of reduced translation and increased chaperone, ROS generation, protein quality control, and mRNA and protein degradation (48). SST cells showed evidence of all such changes, driven by elevated *Hspa5*, the primary molecular sensor of misfolded proteins, which activates the unfolded protein response, one arm of the ER stress response (48–50). This finding replicates previous work showing increased unfolded protein response in SST cells after UCMS exposure (21). Epidermal growth factor, platelet-derived growth factor, and FGF are neurotrophic in the adult central nervous system, and their inhibition or abolishment has negative cellular and behavioral consequences (51–55). Although reduced BDNF (brain-derived neurotrophic factor) is traditionally implicated in

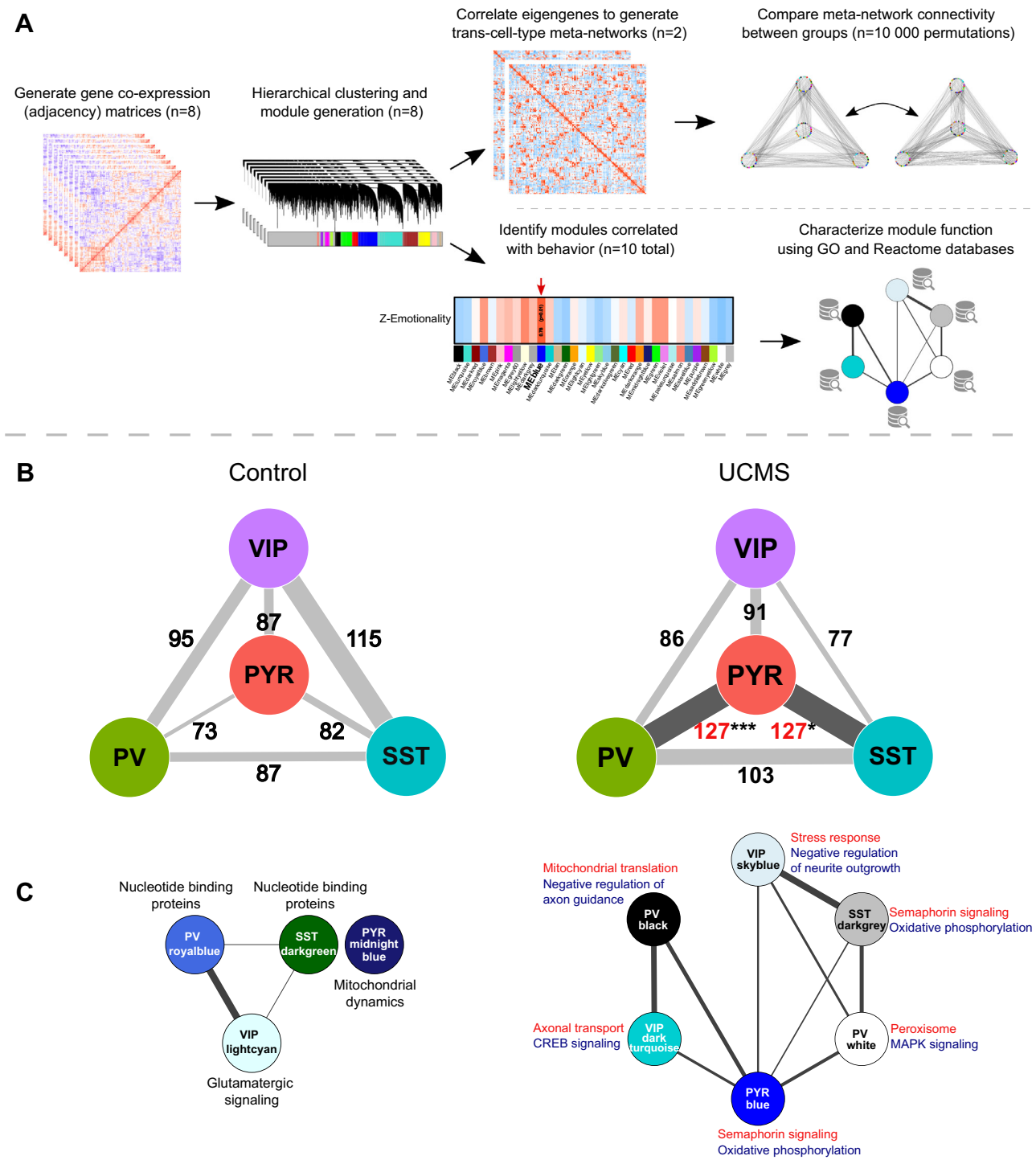

Figure 4. UCMS strengthens transcriptome-wide coexpression between PYR cells and both SST and PV cells. **(A)** Analytic workflow used in coexpression analyses. **(B)** Transcriptome-wide coexpression patterns in control (left) and UCMS (right) groups. Weighted gene coexpression network analysis modules generated within cell types were correlated, generating a transcell-type metanetwork. Edges between cell types represent the number of significant pairwise correlations between module eigengenes. Counts in black showed no significant differences between groups; those in red showed a significant increase in coexpression in UCMS. Statistical significance was calculated by permutation test (n = 10,000) of weighted gene coexpression network analysis results. *$p < .05$, ***$p < .001$. **(C)** Subnetwork of weighted gene coexpression network analysis modules significantly correlated to behavior in control (left) and UCMS (right) groups. Labels indicate biological functions most significantly enriched in each module using Enrichr. In the UCMS subnetwork, functions enriched in upregulated genes are shown in red, and downregulated genes in blue. CREB, cAMP-response element binding protein; GO, gene ontology; MAPK, mitogen-activated protein kinase; PV, parvalbumin; PYR, pyramidal; SST, somatostatin; UCMS, unpredictable chronic mild stress; VIP, vasoactive intestinal peptide.

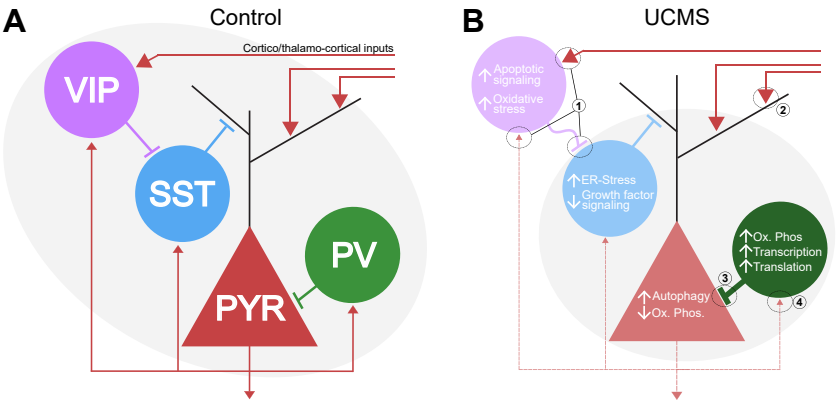

Figure 5. Predicted consequences of UCMS-induced cell type–specific transcriptomic changes on cortical microcircuit function. **(A)** A control (healthy) cortical microcircuit maintains excitation-inhibition balance and normal information processing through recruitment and involvement of all cell types (gray outline), where regulation of excitatory input by VIP and SST cells is balanced by PV cell–mediated output regulation, ensuring appropriate detection, processing, and transfer of PYR cell–mediated excitatory information. **(B)** UCMS induces a structural and functional reorganization of the cortical microcircuit, characterized by perturbations in all cell types. Transcriptomic responses displayed coordinated changes across PYR, PV, and SST cells (gray shading), suggesting an organized recruitment of these cell types. Intracellular signaling changes, coupled with synaptic changes, suggest decreased activity of PYR, SST, and VIP cells and increased PV cell activity: 1) aberrant axonal and dendritic expression in VIP cells compromises proper integration of corticocortical and feedback inputs, in addition to impaired transmission of inhibitory signals to SST cells; 2) decreased glutamatergic receptor complexes in PYR cells reduces response to corticocortical and thalamocortical inputs; 3) increased axonal microtubule and cytoskeletal gene expression, along with increased biosynthesis, suggest increased inhibition of PYR cells; 4) decreased postsynaptic glutamatergic complexes in PV cells suggest decreased feedback signaling by PYR cells, aside from the general decrease in PYR cell presynaptic gene expression. These changes may manifest as decreased VIP/SST-mediated input and increased PV-mediated output regulation of PYR cells, consequently maintaining the excitation-inhibition balance but potentially negatively affecting the coding and integrity of neural information. ER, endoplasmic reticulum; Ox. Phos., oxidative phosphorylation; PV, parvalbumin; PYR, pyramidal; SST, somatostatin; UCMS, unpredictable chronic mild stress; VIP, vasoactive intestinal peptide.

chronic stress and MDD (13,56–58), these other growth factor pathways may represent additional and/or alternate neurotrophic deficits. Platelet-derived growth factor and FGF are involved in synaptic plasticity and regulation of NMDA receptor activation, and reduction or abolishment of FGF induces anxiety- and anhedonia-like behavior (51–55). These signaling pathways also contribute to determining GABAergic and glutamatergic cell fates (55,59,60), and reduced function may contribute to loss of cellular identity, similar to natural aging (61). Overall, SST cells show reduced cellular integrity, suggestive of a decreased capacity to provide continuous PYR cell dendritic inhibition.

PV cells were characterized by downregulated postsynaptic receptors, CAMs, and potassium channel expression and upregulated mitochondrial function, biosynthetic pathways, and microtubule dynamics. Decreased glutamatergic receptor subunits, scaffolding genes (including *Gria1* and *Dlgap4*), and AMPA-associated K^+ channels (*Kcnt1*), in addition to decreased postsynaptic CAM expression, suggest reduced excitatory input from PYR cells, consistent with observations of presynaptic deficits in PYR cells and reports of reduced excitatory inputs onto PV cells of mice with elevated behavioral emotionality (62). Moreover, axonal microtubule polymerization, stabilization, and anterograde transport were increased, suggestive of axonogenesis and synaptogenesis (63,64). Indeed, these findings are consistent with reports of increased PV cell excitability, activity, and axonal extension and myelination after UCMS (65,66). Taken together, these findings suggest that PV cells may increase axonal arborization targeting PYR cells. However, overall PV cell findings must be tempered by the reality of relatively few differentially expressed genes. In summary, although PV cells show reduced excitatory inputs, presynaptic changes suggest increased inhibitory function.

Finally, VIP cells appeared to show compromised pre- and postsynaptic structure and function, in addition to decreased cellular integrity and neurotrophic signaling. In enrichment analyses, VIP cells showed deficits in postsynaptic CAMs and dendritic structure genes, consistent with presynaptic PYR cell deficits. Downregulated axonal structure and vesicle release genes would likewise suggest reduced inhibition of SST cells. These findings may reflect adaptations of VIP cells to reduced PYR and SST cell function or consequences of cellular stress and apoptotic signaling. Although less robust than synaptic-related changes, apoptotic signaling is observed in bulk RNA-seq of the medial PFC in UCMS (42,67). Despite VIP cells constituting 3% to 4% of cortical cells, naturally low apoptotic signaling may be detectable in bulk tissue if increased in a low-abundance cell type (5). Finally, VIP cell densities were unchanged (Figure S3 in Supplement 1), precluding actual cell death. Increased apoptotic signaling and oxidative stress in VIP cells may contribute to reduced cell function, consistent with previous reports of reduced VIP peptide expression in UCMS (28), perhaps leading to impaired regulation of SST cells.

Predicted Implications for Overall Cortical Microcircuit Information Processing

The DE and coexpression results suggest a shift in microcircuit EIB toward a lower level of overall activity (Figure 5), characterized first by reduced PYR cell activity. Reduced SST cell function suggests decreased input regulation of PYR cells, whereas increased PV cell function suggests increased output control, together predicted to increase basal and maintain activity-dependent firing of PYC cells, resulting in decreased signal-to-noise ratio of PYR cells necessary for information processing (23). VIP cells showed no coordinated changes with other cell types, although our findings suggested impaired function of these cells. VIP cells act as a cellular switch, regulating SST cells to either integrate or cancel dendritic PYR cell inputs, and impaired function would contribute to

mistiming of SST cell inhibition with incoming excitatory inputs (68–71). Moreover, tighter PV-mediated control of excitatory outputs, while potentially compensating for reduced SST cell inhibition, may result in a less flexible microcircuit that is unable to filter spurious and noisy inputs. In summary, although based on mRNA measures, these findings suggest a shift in microcircuit EIB to lower activity levels and impaired PYR cell input regulation, implicating a corruption in mood-relevant information processing in the medial PFC.

Limitations and Future Studies

This study is not without limitations. First, only male mice were used, precluding conclusions about effects in females. Depression disproportionately affects females and recent bulk and cell-specific RNA-seq studies in UCMS suggest that 1) male and female depressive transcriptomes are different (18,72–74) and 2) female mice may have innate deficiencies in unfolded protein response signaling (75). These findings highlight the importance of studies in female mice, determining if the above sex differences show cell specificity. Second, mice received 5 weeks of UCMS; thus, these transcriptomic changes represent both stress-induced cellular responses and compensatory adaptations of other cell types because the cross-sectional data cannot assess the sequence of cellular deficits. Third, contamination by off-target cell types had the potential to skew results by introducing mRNA from other astrocytes, oligodendrocytes, microglia, and other neurons. However, Figure S4 in Supplement 1 demonstrates that molecular markers of contamination were expressed at very low levels (e.g., >50-fold lower than *Sst*). Fourth, our sample size was moderate (n = 10/group), although comparable to other mouse RNA-seq studies (42,67,76,77). Finally, the cell types investigated are not fully unique, and further divisions of SST and PV cells, for instance, can be made (4,78).

Future studies should focus on replicating our cell type–specific and microcircuit-wide findings, including at the electrophysiological level; investigate time courses of changes; and narrow our results for potential antidepressant modalities. Because we found that cell types respond uniquely to UCMS, future studies should also determine the cell type–specific effects of existing and novel antidepressants on transcriptional profiles, particularly those with synaptic effects, such as ketamine.

ACKNOWLEDGMENTS AND DISCLOSURES

This work was supported by a Canadian Institute of Health Research Project Scheme Grant (Grant No. PJT-153175 [to ES]). DFN was supported by funding provided by the Ontario Graduate Scholarship and Brain Canada, in partnership with Health Canada, for the Canadian Open Neuroscience Platform initiative. CF was supported by a CAMH Discovery Fund fellowship and Ontario Graduate Scholarship during the studies. MB is supported by a NARSAD young investigator award from the Brain & Behavior Research Foundation (Grant No. 24034) and the CAMH Discovery Seed Fund and the Canadian Institutes of Health Research (Grant No. PJT-165852). This work was also supported by the Campbell Family Mental Health Research Institute (to ES).

DFN performed brain sectioning, RNAscope–laser capture microdissection collection of cell types, cell densitometry staining and microscopy, bioinformatics, statistical analysis, and wrote the manuscript. HO performed library preparation, quantitative microscopy, and associated image analysis and provided input into analytic strategies. RS assisted with bioinformatic analyses and methods refinement and provided input into analytic strategies. KM and CF performed unpredictable chronic mild stress procedures and behavioral tests. MB oversaw and coordinated animal procedures. ES conceptualized the study and provided funding. All authors contributed to manuscript review.

We thank the Centre for Addiction and Mental Health Sequencing Facility for assistance running the Illumina HiSeq2500 platform and Gary Bader for input on coexpression analyses. Coexpression computations were performed on the CAMH Specialized Computing Cluster. The Specialized Computing Cluster is funded by the Canada Foundation for Innovation, Research Hospital Fund. We thank Netta Ussyshkin for help with cell densitometry studies.

A previous version of this article was published as a preprint on bioRxiv: https://doi.org/10.1101/2020.08.18.249995. A number of analytic differences exist between this manuscript and the bioRxiv version.

ES is founder and Acting Chief Scientific Officer of Damona Pharmaceuticals, a drug development company with small molecules in the pipeline for treatment of cognitive deficits across brain disorders and aging. All other authors report no biomedical financial interests or potential conflicts of interest.

ARTICLE INFORMATION

From the Department of Pharmacology and Toxicology (DFN, KM, CF, MB, ES) and Department of Psychiatry (ES), University of Toronto; Campbell Family Mental Health Research Institute of the Centre of Addiction and Mental Health (DFN, HO, RS, KM, CF, MB, ES), Toronto, Ontario, Canada; and Department of Neurosciences (RS), University of Toledo, Toledo, Ohio.

DFN and HO contributed equally to this work.

Address correspondence to Etienne Sibille, Ph.D., at Etienne.sibille@camh.ca.

Received Aug 17, 2021; revised Sep 29, 2021; accepted Oct 13, 2021.

Supplementary material cited in this article is available online at https://doi.org/10.1016/j.biopsych.2021.10.015.

REFERENCES

1. Hasin DS, Sarvet AL, Meyers JL, Saha TD, Ruan WJ, Stohl M, Grant BF (2018): Epidemiology of adult DSM-5 major depressive disorder and its specifiers in the United States. JAMA Psychiatry 75:336–346.
2. American Psychiatric Association (2013): Diagnostic and Statistical Manual of Mental Disorders, 5th ed. Washington, DC: American Psychiatric Publishing.
3. Prins J, Olivier B, Korte SM (2011): Triple reuptake inhibitors for treating subtypes of major depressive disorder: The monoamine hypothesis revisited. Expert Opin Investig Drugs 20:1107–1130.
4. Tasic B, Yao Z, Graybuck LT, Smith KA, Nguyen TN, Bertagnolli D, *et al.* (2018): Shared and distinct transcriptomic cell types across neocortical areas. Nature 563:72–78.
5. Tremblay R, Lee S, Rudy B (2016): GABAergic interneurons in the neocortex: From cellular properties to circuits. Neuron 91:260–292.
6. Northoff G, Sibille E (2014): Cortical GABA neurons and self-focus in depression: A model linking cellular, biochemical and neural network findings. Mol Psychiatry 19:959.
7. Xue M, Atallah BV, Scanziani M (2014): Equalizing excitation-inhibition ratios across visual cortical neurons. Nature 511:596–600.
8. Fee C, Banasr M, Sibille E (2017): Somatostatin-positive gamma-aminobutyric acid interneuron deficits in depression: Cortical microcircuit and therapeutic perspectives. Biol Psychiatry 82:549–559.
9. Agid Y, Buzsáki G, Diamond DM, Frackowiak R, Giedd J, Girault JA, *et al.* (2007): How can drug discovery for psychiatric disorders be improved? Nat Rev Drug Discov 6:189–201.
10. Levinson AJ, Fitzgerald PB, Favalli G, Blumberger DM, Daigle M, Daskalakis ZJ (2010): Evidence of cortical inhibitory deficits in major depressive disorder. Biol Psychiatry 67:458–464.
11. Schür RR, Draisma LWR, Wijnen JP, Boks MP, Koevoets MGJC, Joëls M, *et al.* (2016): Brain GABA levels across psychiatric disorders: A systematic literature review and meta-analysis of (1) H-MRS studies. Hum Brain Mapp 37:3337–3352.

12. Choudary PV, Molnar M, Evans SJ, Tomita H, Li JZ, Vawter MP, *et al.* (2005): Altered cortical glutamatergic and GABAergic signal transmission with glial involvement in depression. Proc Natl Acad Sci U S A 102:15653–15658.
13. Chang LC, Jamain S, Lin CW, Rujescu D, Tseng GC, Sibille E (2014): A conserved BDNF, glutamate- and GABA-enriched gene module related to human depression identified by coexpression meta-analysis and DNA variant genome-wide association studies. PLoS One 9: e90980.
14. Kang HJ, Adams DH, Simen A, Simen BB, Rajkowska G, Stockmeier CA, *et al.* (2007): Gene expression profiling in postmortem prefrontal cortex of major depressive disorder. J Neurosci 27:13329–13340.
15. Nagy C, Maitra M, Tanti A, Suderman M, Théroux JF, Davoli MA, *et al.* (2020): Single-nucleus transcriptomics of the prefrontal cortex in major depressive disorder implicates oligodendrocyte precursor cells and excitatory neurons. Nat Neurosci 23:771–781.
16. Douillard-Guilloux G, Lewis D, Seney ML, Sibille E (2017): Decrease in somatostatin-positive cell density in the amygdala of females with major depression. Depress Anxiety 34:68–78.
17. Seney ML, Tripp A, McCune S, Lewis DA, Sibille E (2015): Laminar and cellular analyses of reduced somatostatin gene expression in the subgenual anterior cingulate cortex in major depression. Neurobiol Dis 73:213–219.
18. Tripp A, Kota RS, Lewis DA, Sibille E (2011): Reduced somatostatin in subgenual anterior cingulate cortex in major depression. Neurobiol Dis 42:116–124.
19. Piantadosi SC, French BJ, Poe MM, Timić T, Marković BD, Pabba M, *et al.* (2016): Sex-dependent anti-stress effect of an α5 subunit containing $GABA_A$ receptor positive allosteric modulator. Front Pharmacol 7:446.
20. Sun HL, Zhou ZQ, Zhang GF, Yang C, Wang XM, Shen JC, *et al.* (2016): Role of hippocampal p11 in the sustained antidepressant effect of ketamine in the chronic unpredictable mild stress model. Transl Psychiatry 6:e741.
21. Lin LC, Sibille E (2015): Somatostatin, neuronal vulnerability and behavioral emotionality. Mol Psychiatry 20:377–387.
22. Fino E, Yuste R (2011): Dense inhibitory connectivity in neocortex. Neuron 69:1188–1203.
23. Prévot T, Sibille E (2021): Altered GABA-mediated information processing and cognitive dysfunctions in depression and other brain disorders. Mol Psychiatry 26:151–167.
24. Duman RS, Sanacora G, Krystal JH (2019): Altered connectivity in depression: GABA and glutamate neurotransmitter deficits and reversal by novel treatments. Neuron 102:75–90.
25. Kang HJ, Voleti B, Hajszan T, Rajkowska G, Stockmeier CA, Licznerski P, *et al.* (2012): Decreased expression of synapse-related genes and loss of synapses in major depressive disorder. Nat Med 18:1413–1417.
26. Li N, Liu RJ, Dwyer JM, Banasr M, Lee B, Son H, *et al.* (2011): Glutamate N-methyl-D-aspartate receptor antagonists rapidly reverse behavioral and synaptic deficits caused by chronic stress exposure. Biol Psychiatry 69:754–761.
27. Duman RS, Aghajanian GK, Sanacora G, Krystal JH (2016): Synaptic plasticity and depression: New insights from stress and rapid-acting antidepressants. Nat Med 22:238–249.
28. Banasr M, Lepack A, Fee C, Duric V, Maldonado-Aviles J, DiLeone R, *et al.* (2017): Characterization of GABAergic marker expression in the chronic unpredictable stress model of depression. Chronic Stress (Thousand Oaks) 1:2470547017720459.
29. Northoff G, Sibille E (2014): Why are cortical GABA neurons relevant to internal focus in depression? A cross-level model linking cellular, biochemical and neural network findings. Mol Psychiatry 19:966–977.
30. Nikolova YS, Misquitta KA, Rocco BR, Prevot TD, Knodt AR, Ellegood J, *et al.* (2018): Shifting priorities: Highly conserved behavioral and brain network adaptations to chronic stress across species. Transl Psychiatry 8:26.
31. Paxinos G, Franklin KBJ (2012): The Mouse Brain in Stereotaxic Coordinates, 4th ed. Cambridge: Academic Press.
32. Rocco BR, Oh H, Shukla R, Mechawar N, Sibille E (2017): Fluorescence-based cell-specific detection for laser-capture microdissection in human brain. Sci Rep 7:14213.
33. Shukla R, Prevot TD, French L, Isserlin R, Rocco BR, Banasr M, *et al.* (2019): The relative contributions of cell-dependent cortical microcircuit aging to cognition and anxiety. Biol Psychiatry 85:257–267.
34. Langfelder P, Horvath S (2008): WGCNA: An R package for weighted correlation network analysis. BMC Bioinformatics 9:559.
35. Love MI, Huber W, Anders S (2014): Moderated estimation of fold change and dispersion for RNA-seq data with DESeq2. Genome Biol 15:550.
36. Subramanian A, Tamayo P, Mootha VK, Mukherjee S, Ebert BL, Gillette MA, *et al.* (2005): Gene set enrichment analysis: A knowledge-based approach for interpreting genome-wide expression profiles. Proc Natl Acad Sci U S A 102:15545–15550.
37. Guilloux JP, Douillard-Guilloux G, Kota R, Wang X, Gardier AM, Martinowich K, *et al.* (2012): Molecular evidence for BDNF- and GABA-related dysfunctions in the amygdala of female subjects with major depression. Mol Psychiatry 17:1130–1142.
38. Lalovic A, Klempan T, Sequeira A, Luheshi G, Turecki G (2010): Altered expression of lipid metabolism and immune response genes in the frontal cortex of suicide completers. J Affect Disord 120:24–31.
39. Klempan TA, Sequeira A, Canetti L, Lalovic A, Ernst C, ffrench-Mullen J, Turecki G (2009): Altered expression of genes involved in ATP biosynthesis and GABAergic neurotransmission in the ventral prefrontal cortex of suicides with and without major depression. Mol Psychiatry 14:175–189.
40. McEwen BS, Bowles NP, Gray JD, Hill MN, Hunter RG, Karatsoreos IN, Nasca C (2015): Mechanisms of stress in the brain. Nat Neurosci 18:1353–1363.
41. Bansal Y, Kuhad A (2016): Mitochondrial dysfunction in depression. Curr Neuropharmacol 14:610–618.
42. Tordera RM, Garcia-García AL, Elizalde N, Segura V, Aso E, Venzala E, *et al.* (2011): Chronic stress and impaired glutamate function elicit a depressive-like phenotype and common changes in gene expression in the mouse frontal cortex. Eur Neuropsychopharmacol 21:23–32.
43. Lee JA (2012): Neuronal autophagy: A housekeeper or a fighter in neuronal cell survival? Exp Neurobiol 21:1–8.
44. Tomoda T, Yang K, Sawa A (2020): Neuronal autophagy in synaptic functions and psychiatric disorders. Biol Psychiatry 87:787–796.
45. Sumitomo A, Yukitake H, Hirai K, Horike K, Ueta K, Chung Y, *et al.* (2018): Ulk2 controls cortical excitatory-inhibitory balance via autophagic regulation of p62 and GABAA receptor trafficking in pyramidal neurons. Hum Mol Genet 27:3165–3176.
46. Gassen NC, Rein T (2019): Is there a role of autophagy in depression and antidepressant action? Front Psychiatry 10:337.
47. Moda-Sava RN, Murdock MH, Parekh PK, Fetcho RN, Huang BS, Huynh TN, *et al.* (2019): Sustained rescue of prefrontal circuit dysfunction by antidepressant-induced spine formation. Science 364: eaat8078.
48. Hetz C (2012): The unfolded protein response: Controlling cell fate decisions under ER stress and beyond. Nat Rev Mol Cell Biol 13:89–102.
49. Bertolotti A, Zhang Y, Hendershot LM, Harding HP, Ron D (2000): Dynamic interaction of BiP and ER stress transducers in the unfolded-protein response. Nat Cell Biol 2:326–332.
50. Lee AS (2005): The ER chaperone and signaling regulator GRP78/BiP as a monitor of endoplasmic reticulum stress. Methods 35:373–381.
51. Yamanaka Y, Kitano A, Takao K, Prasansuklab A, Mushiroda T, Yamazaki K, *et al.* (2011): Inactivation of fibroblast growth factor binding protein 3 causes anxiety-related behaviors. Mol Cell Neurosci 46:200–212.
52. Birey F, Kloc M, Chavali M, Hussein I, Wilson M, Christoffel D, *et al.* (2015): Genetic and stress-induced loss of NG2 glia triggers emergence of depressive-like behaviors through reduced secretion of FGF2 [published correction appears in Neuron 2019; 104:825–826. Neuron 88:941–956.
53. Brooks LR, Enix CL, Rich SC, Magno JA, Lowry CA, Tsai PS (2014): Fibroblast growth factor deficiencies impact anxiety-like behavior and the serotonergic system. Behav Brain Res 264:74–81.

54. Di Re J, Wadsworth PA, Laezza F (2017): Intracellular fibroblast growth factor 14: Emerging risk factor for brain disorders. Front Cell Neurosci 11:103.
55. Funa K, Sasahara M (2014): The roles of PDGF in development and during neurogenesis in the normal and diseased nervous system. J Neuroimmune Pharmacol 9:168–181.
56. Duman RS (2014): Neurobiology of stress, depression, and rapid acting antidepressants: Remodeling synaptic connections. Depress Anxiety 31:291–296.
57. Oh H, Piantadosi SC, Rocco BR, Lewis DA, Watkins SC, Sibille E (2019): The role of dendritic brain-derived neurotrophic factor transcripts on altered inhibitory circuitry in depression. Biol Psychiatry 85:517–526.
58. Tripp A, Oh H, Guilloux JP, Martinowich K, Lewis DA, Sibille E (2012): Brain-derived neurotrophic factor signaling and subgenual anterior cingulate cortex dysfunction in major depressive disorder. Am J Psychiatry 169:1194–1202.
59. Garcez RC, Teixeira BL, Schmitt Sdos S, Alvarez-Silva M, Trentin AG (2009): Epidermal growth factor (EGF) promotes the in vitro differentiation of neural crest cells to neurons and melanocytes. Cell Mol Neurobiol 29:1087–1091.
60. Stevens HE, Smith KM, Maragnoli ME, Fagel D, Borok E, Shanabrough M, *et al.* (2010): FGFR2 is required for the development of the medial prefrontal cortex and its connections with limbic circuits. J Neurosci 30:5590–5602.
61. Goh JOS (2011): Functional dedifferentiation and altered connectivity in older adults: Neural accounts of cognitive aging. Aging Dis 2:30–48.
62. Perova Z, Delevich K, Li B (2015): Depression of excitatory synapses onto parvalbumin interneurons in the medial prefrontal cortex in susceptibility to stress. J Neurosci 35:3201–3206.
63. Mattson MP, Gleichmann M, Cheng A (2008): Mitochondria in neuroplasticity and neurological disorders. Neuron 60:748–766.
64. Chang DTW, Reynolds IJ (2006): Differences in mitochondrial movement and morphology in young and mature primary cortical neurons in culture. Neuroscience 141:727–736.
65. Page CE, Shepard R, Heslin K, Coutellier L (2019): Prefrontal parvalbumin cells are sensitive to stress and mediate anxiety-related behaviors in female mice. Sci Rep 9:19772.
66. Stedehouder J, Brizee D, Shpak G, Kushner SA (2018): Activity-dependent myelination of parvalbumin interneurons mediated by axonal morphological plasticity. J Neurosci 38:3631–3642.
67. Liu Y, Yang N, Zuo P (2010): cDNA microarray analysis of gene expression in the cerebral cortex and hippocampus of BALB/c mice subjected to chronic mild stress. Cell Mol Neurobiol 30:1035–1047.
68. Pi HJ, Hangya B, Kvitsiani D, Sanders JI, Huang ZJ, Kepecs A (2013): Cortical interneurons that specialize in disinhibitory control. Nature 503:521–524.
69. Cardin JA (2018): Inhibitory interneurons regulate temporal precision and correlations in cortical circuits. Trends Neurosci 41:689–700.
70. Williams LE, Holtmaat A (2019): Higher-order thalamocortical inputs gate synaptic long-term potentiation via disinhibition. Neuron 101:91–102.e4.
71. Hertäg L, Sprekeler H (2019): Amplifying the redistribution of somatodendritic inhibition by the interplay of three interneuron types. PLoS Comput Biol 15:e1006999.
72. Paden W, Barko K, Puralewski R, Cahill KM, Huo Z, Shelton MA, *et al.* (2020): Sex differences in adult mood and in stress-induced transcriptional coherence across mesocorticolimbic circuitry. Transl Psychiatry 10:59.
73. Seney ML, Huo Z, Cahill K, French L, Puralewski R, Zhang J, *et al.* (2018): Opposite molecular signatures of depression in men and women. Biol Psychiatry 84:18–27.
74. Labonté B, Engmann O, Purushothaman I, Menard C, Wang J, Tan C, *et al.* (2017): Sex-specific transcriptional signatures in human depression. Nat Med 23:1102–1111.
75. Gerhard DM, Pothula S, Liu RJ, Wu M, Li XY, Girgenti MJ, *et al.* (2020): GABA interneurons are the cellular trigger for ketamine's rapid antidepressant actions. J Clin Invest 130:1336–1349.
76. Laine MA, Trontti K, Misiewicz Z, Sokolowska E, Kulesskaya N, Heikkinen A, *et al.* (2018): Genetic control of myelin plasticity after chronic psychosocial stress. eNeuro 5.. ENEURO.0166-18.2018.
77. Manners MT, Yohn NL, Lahens NF, Grant GR, Bartolomei MS, Blendy JA (2019): Transgenerational inheritance of chronic adolescent stress: Effects of stress response and the amygdala transcriptome. Genes Brain Behav 18:e12493.
78. Tasic B, Menon V, Nguyen TN, Kim TK, Jarsky T, Yao Z, *et al.* (2016): Adult mouse cortical cell taxonomy revealed by single cell transcriptomics. Nat Neurosci 19:335–346.